PTEP

Prog. Theor. Exp. Phys. **2025** 023H04 (11 pages)
DOI: 10.1093/ptep/ptaf007

Removal of Radioactive Noble Gas Radon from Air by Ag-Zeolite

H. Ogawa[1,*], Y. Takeuchi[2,3], H. Sekiya[3,4], K. Iyoki[5], M. Matsukura[6], T. Wakihara[6,7], Y. Nakano[8], S. Hirano[9], and A. Taniguchi[10]

[1]*College of Science and Technology, Nihon University, 1-8-14 Kanda, Surugadai, Chiyoda-ku, Tokyo 180-0011, Japan*
[2]*Department of Physics, Graduate School of Science, Kobe University, 1-1 Rokkodai, Noda, Kobe, Hyogo 657-8501, Japan*
[3]*Kavli Institute for the Physics and Mathematics of the Universe (WPI), The University of Tokyo Institutes for Advanced Study, University of Tokyo, 5-1-5 Kashiwanoha, Kashiwa, Chiba 277-8583, Japan*
[4]*Kamioka Observatory, Institute for Cosmic Ray Research, University of Tokyo, 456 Higashi Mozumi, Kamioka, Gifu 506-1205, Japan*
[5]*Department of Environment Systems, The University of Tokyo, 5-1-5 Kashiwanoha, Kashiwa-shi, Chiba 277-8563, Japan*
[6]*Institute of Engineering Innovation,School of Engineering, The University of Tokyo, 7-3-1 Hongo, Bunkyo-ku, Tokyo 113-8656, Japan*
[7]*Department of Chemical System Engineering, The University of Tokyo, 7-3-1 Hongo, Bunkyo, Tokyo 113-8656, Japan*
[8]*Faculty of Science, University of Toyama, Gofuku, Toyama-shi, Toyama 930-8555, Japan*
[9]*Tosoh Corporation , 2-2-1 Yaesu, Chuo, Tokyo 104-8467, Japan*
[10]*Sinanen Zeomic Co., Ltd, Nakagawa-honmachi, Minato, Nagoya, Aichi 455-0051, Japan*
*Email: ogawa.hiroshi@nihon-u.ac.jp

Received November 6, 2024; Revised January 2, 2025; Accepted January 15, 2025; Published January 16, 2025

This paper investigates the removal of radon from purified and ambient airs by Ag-zeolite. Ag-zeolite is known to have very high performance in terms of airborne radon removal. The dependence on zeolite type and silver content of the performance of radon removal was evaluated. The performance of radon removal by a single pass and radon emanation were also evaluated. In addition, the adsorption performance due to zeolite solidification and the change in adsorption performance due to moisture in the gas were evaluated in order to investigate properties that should be considered for future practical use. These properties will be applicable to the development of air purification systems for large-volume ultra-low-radioactivity experiments.

Subject Index H20

1. Introduction

Neutrino experiments and direct dark matter search experiments require an extremely low radioactivity environment at the facility where the experimental detectors are constructed [1]. In particular, radioactive radon gas in the air must be reduced to the utmost limit because it generates radioactivity from the rocks in the underground facility and the detector itself. Radon is produced from radioactive impurities of members of the uranium and thorium series in bedrock. Radiation from the beta decay of ^{214}Bi, the daughter nucleus of ^{222}Rn, puts a limit on the observed energy threshold for solar neutrino observations in a water Cherenkov detector, such as Super-Kamiokande [2–4]. In addition, beta radiation from ^{214}Pb, which is the

daughter nucleus of ^{222}Rn, and nuclear recoil from alpha decay of ^{210}Po, which attaches to the detector surface, can be background events in low-energy solar neutrino and dark matter search experiments.

Airborne radon removal has been done at these extremely low radioactivity experimental facilities. But in recent years, as experimental facilities have become larger, the development of more efficient radon removal equipment has been demanded. For example, the Hyper-Kamiokande water Cherenkov detector under construction in Hida City, Gifu Prefecture, Japan [5], is of a larger size than Super-Kamiokande, requiring 3 times the processing capacity of the air purification system that used to use activated carbon to aim toward 1 mBq/m^3 radon concentration [6,7].

A promising adsorbent with even better radon adsorption capacity is silver (Ag) ion-exchanged zeolite (Ag-zeolite). Ag-zeolite can be prepared by an ion-exchange process that introduces Ag ions into the zeolite pore structure. Gases are adsorbed by chemisorption through the interaction of Ag ions and electrons of gas. Adsorption technology using Ag-zeolite has been studied extensively in recent years [8]. In addition, Ag-zeolite was found to have excellent radon adsorption performance. Ag-zeolite retains its radon adsorption capacity even at room temperature [9,10]. Therefore, it is expected to be useful in developing an air purification system that is less expensive, compact, and can be operated at room temperature. The use of Ag-zeolite as a purification device for ultra-low-radioactivity experiments is a new idea that has not yet been put to practical use.

In this paper, samples of Ag-zeolites were fabricated and their adsorption performance on radon in air was investigated. Two types of base zeolites and samples with different exchange ratios of Ag ions were investigated as Ag-zeolites. The emanation of radon, the effect of moisture, and the effect of solidification were also investigated. Then, prospects for the development of a new air purification system are discussed.

2. Synthesis of the Ag-zeolite

Three different Ag-zeolite samples were prepared, derived from two base zeolites: Zeolite Socony Mobil–5 [MFI-type zeolite, $SiO_2/Al_2O_3 \sim 40$ (mol/mol)] and Ferrierite [FER-type zeolite $SiO_2/Al_2O_3 \sim 18$ (mol/mol)]. We selected these zeolites because the aluminum content (Al/Si) in the zeolite that is actually in the form of an ion-compound with silver is relatively large. These bases were in Na form and were ion-exchanged to Ag in AgCl solution. In particular, for FER, we prepared samples with Ag loading amounts of 3.0 wt% (Ag-FER3%) and 7.8 wt% (Ag-FER8%). The base zeolite used was a powder purchased from Tosoh Co., and the Ag ion exchange was performed by Sinanen Zeomic Co., Ltd. Furthermore, these samples (Ag-MFI with 3.3 wt% for Ag loading amount, Ag-FER3%, and Ag-FER8%) were pressure solidified by Sinanen Zeomic Co., Ltd. Figure 1 shows a picture of the Ag-MFI sample. These samples were synthesized in June 2023. The amount of samples synthesized was 20 g each. In addition, a sample of MFI zeolite without ion exchange was also prepared.

3. Performance of synthesized Ag-zeolite in gases

3.1. *The radiactivity measurement system and filter housing*

For evaluating the radioactivity removal and intrinsic radioactivity, we used the radioactivity measurement system that is described in detail in Ref. [11]. Figure 2 shows the overview of the

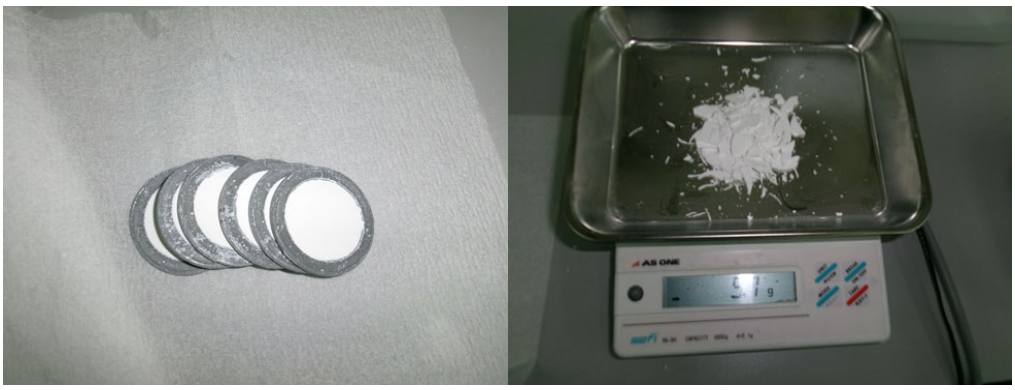

Fig. 1. Photographs of the Ag-MFI zeolite sample. (Left) Solidified sample placed in mold. (Right) A sample being removed from a mold and weighed on a scale.

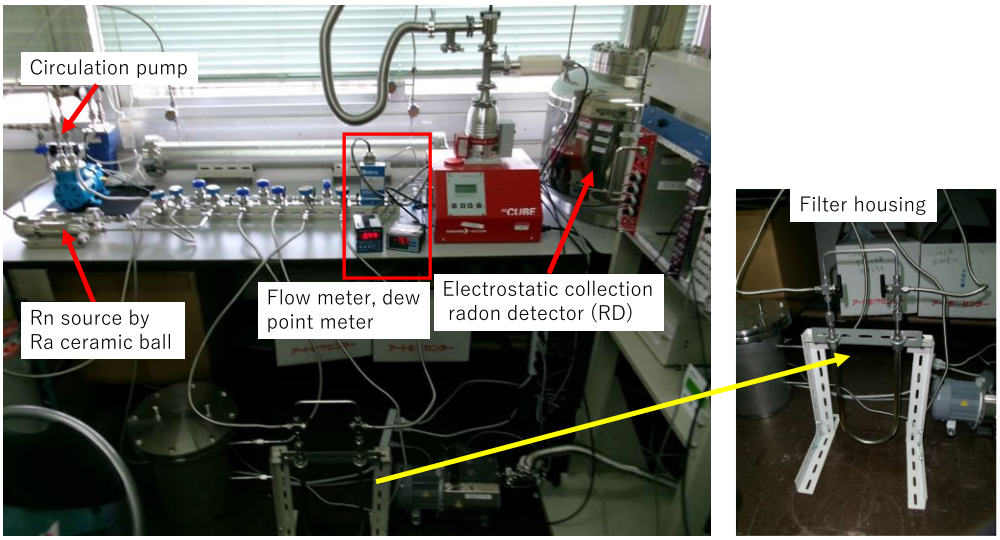

Fig. 2. An overview photograph of the radioactivity measurement system and filter housing (FH). The line setup is a closed system in this photograph.

radioactivity measurement system for this study. The 80 L volume radon detector (RD) with an electrostatic collection was used for the estimation of radon concentration in air, which measures the Rn concentration in gas by detecting alpha-rays from ^{214}Po, the daughter nucleus of ^{222}Rn [12]. The measurement data are recorded in a multichannel analyzer with Raspberry Pi. An air circulation pump (Enomoto Micro Pump Mfg. Co., Ltd., MX-808ST-S) was used to circulate the air. Radium ceramic balls are available as a ^{222}Rn source, and radon can be introduced into the circulated air in advance for radon removal tests. A flow controller (KOFLOC Co. MODEL 5410, 10% accuracy at 0.5 L/min), and a dew point meter (TEKHNE Co. TH-100, $\pm 2^{\circ}$C accuracy) are used to monitor the moisture in the circulating air.

The prepared zeolite was crushed and placed in a filter housing (FH) made of a bent stainless steel pipe, 0.5 inches in diameter and 25 inches in length, as shown in Fig. 2, by following procedure. The actual zeolite-filled length is about 12 inches. The FH has a metal nanoparticle filter (NASclean® GF-T001) in both ends. The FH was activated before the test by heating with a ribbon heater at 350°C for 6 hours with evacuation from both sides of the FH. In the Rn removal test of this study, the FH is placed in a room-temperature environment adjusted to

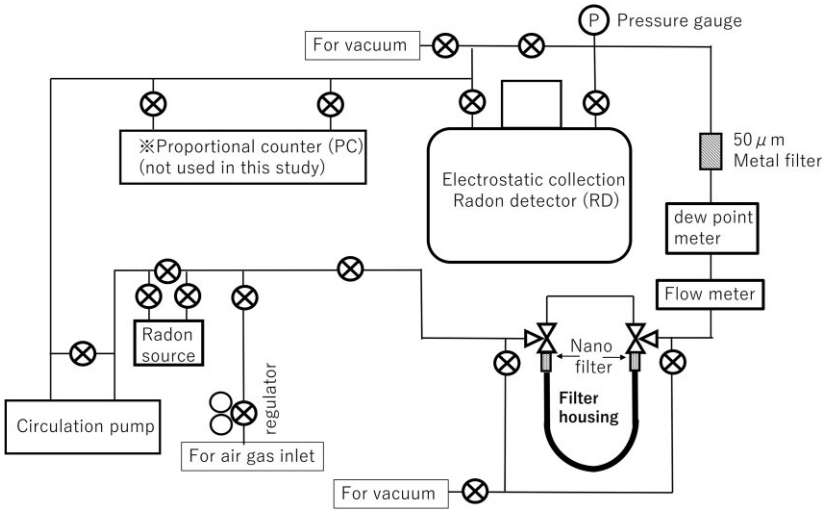

Fig. 3. A schematic representation of the gas line and the radioactivity measurement system for the closed system.

25°C. Here we introduce two flow conditions for two measurements. One is that purified air was circulated between the filter system and RD as a "closed system" for evaluating the retention time of the zeolite. The other is that room air was injected from the filter system to the RD as an "open system" for evaluating the radon removal efficiency under the one-pass situation, which is a similar situation to the actual air purification system for ambient air. These systems will be explained in the following sections.

3.2. *Radon removal measurement by closed system*

The radon removal measurements were conducted with a closed system as follows. Figure 3 shows a schematic representation of the gas line and the radioactivity measurement system for the closed system. Once the RD and the entire line were evacuated, the whole system was filled with commercially available G1-grade high-purity air (impurity concentration < 0.1 ppm) at 1 atm. The circulation of air was then started at 0.5 L/min. Radon was injected from the radon source by passing air gas. After bypassing the radon source, air gas was circulated for about 1 day to ensure a stable radon count rate, estimated by counting the decay of ^{214}Po alpha-rays. Then, the circulating air passes through the filter (filter ON).

Figure 4 shows the time profile of the radon count rate in units of mBq during the radon removal test with an Ag-MFI sample. The radon counting rate decreased suddenly after filter ON, then no radon signal was observed during 50 hours. Then the radon rate slightly recovered after 50 hours.

We compared the radon removal efficiency of three samples. Figure 5 presents the time profiles of the radon reduction factor in the three radon removal tests. The three samples tested in this study showed radon removal on the order of 10^4 at room temperature. This result demonstrates that zeolite has a high radon removal capacity. Figure 5 also shows the radon nonobservation time (RnNO time) for each sample. RnNO time is defined as the time from the disappearance of radon to the appearance of a small amount of radon. Table 1 shows the measurement conditions for each of the three samples and the respective RnNO times. Even though their masses are similar, Ag-FER8% was found to have the longest RnNO time. This indicates that the adsorption rate of radon depends on the Ag content.

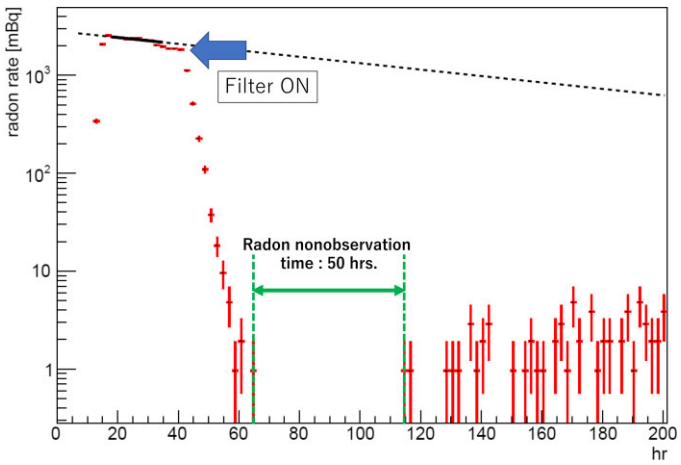

Fig. 4. The time profile of the radon counting rate during the radon removal test with an Ag-MFI sample.

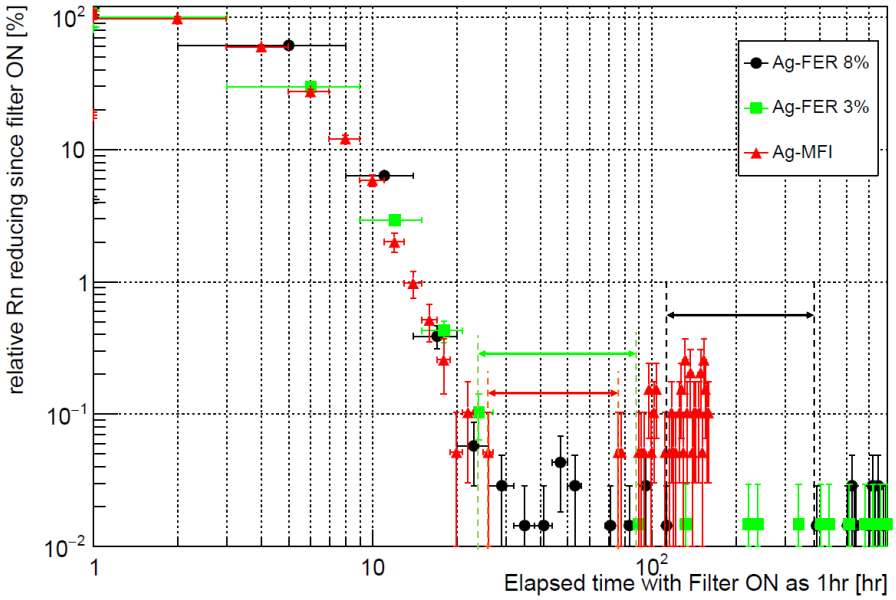

Fig. 5. The time profiles of the radon reduction factor in the three radon removal tests. Black circles, green squares, and red triangles indicate the results for Ag-FER8%, Ag-FER3%, and Ag-MFI, respectively. Each interval and arrow indicates the RnNO time interval for each sample defined in the text.

Table 1. The measurement conditions for each of the three samples and the respective RnNO times in the closed system.

sample name	Ag loading amount [wt%]	sample weight [g]	flow rate [L/min]	RnNO time [hours]
Ag-MFI	3.3	20.9	0.5	50
Ag-FER3%	3.0	20.2	0.5	66
Ag-FER8%	7.8	20.3	0.5	276

3.3. *Radon removal measurement by open system*

In an actual air purification system, it is desirable to remove radon in a single pass through a filter after ambient air is drawn into the system. Therefore, as an initial test in accordance

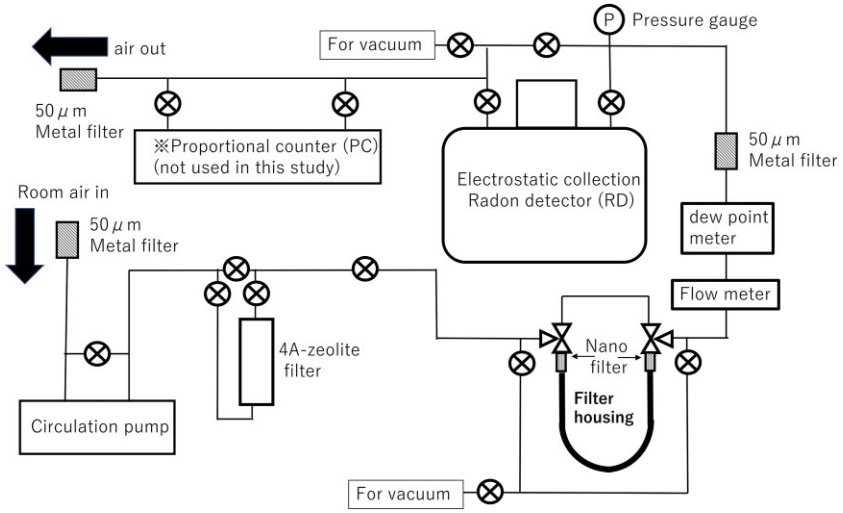

Fig. 6. A schematic representation of the gas line and the radioactivity measurement system for the single-pass system.

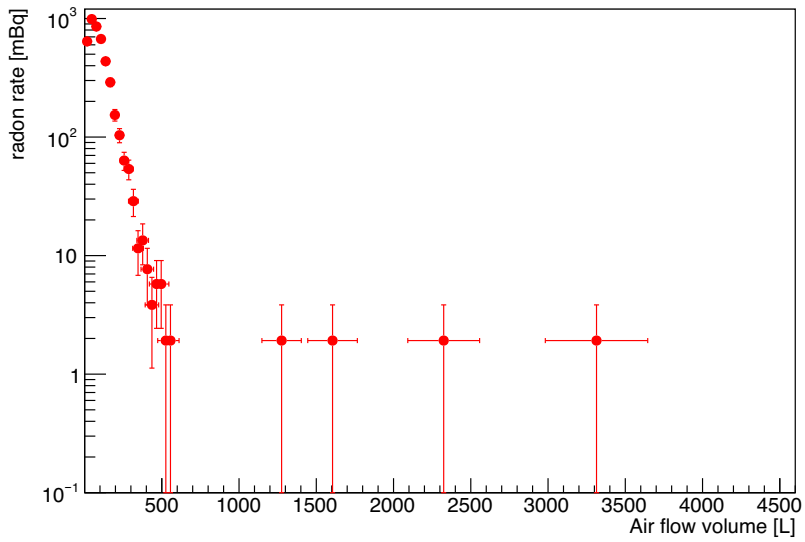

Fig. 7. The time profiles (volume of passing air) of the radon reduction factor in the single-pass test.

with the operation of this actual air purification system, the radon removal measurements were conducted with open flow. Figure 6 shows a schematic representation of the gas line and the radioactivity measurement system for the open system. Indoor air in the laboratory is taken in by a circulation pump at 0.5 L/min. The air is passed through a 200 g of zeolite 4A-type (4A) filter to remove moisture, then through a 20 g Ag-zeolite sample, i.e. Ag-FER8%. Air is released into the room through the RD. For pretreatment of the zeolite, Ag-FER8% underwent the same treatment as that of the previous circulation test, and 4A was baked at 200°C for 2 hours in a thermostatic chamber.

Figure 7 shows the passing air volume profiles (the air flow speed 0.5 L/min × elapsed times to RD) of the radon counting rate in the single-pass test. At the beginning of the measurement (∼0 L in Fig. 7), ambient air was passed only through 4A, and since 4A has no radon adsorption capacity, the Rn counting rate increased. Then, upon passing air through the FH, the radon

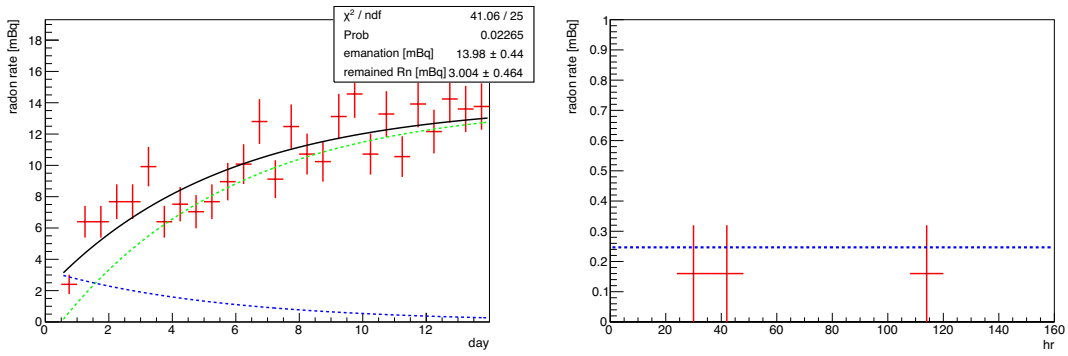

Fig. 8. (Left) The time profile of the radon emanation test with MFI (no Ag ion). The blue dashed line indicates the remaining radon rate and the green dashed line indicates the radon emanation rate. (Right) The time profile of the radon emanation test with Ag-MFI. The blue dashed line indicates the approximate amount of radon emanation due to upwelling from the system, estimated by a separate measurement.

counting rate decreased rapidly. After 1 week of measurement, the nanoparticle filter placed upstream of the 4A became clogged with moisture and impurities, then air flow became zero and the test was stopped. At this point, no increase in radon content was observed, indicating that Ag-FER8% still has sufficient capacity to adsorb radon. It was found that a 20 g Ag-FER8% sample was able to remove radon from at least 4500 L of ambient air in this experiment. The adsorption capacity of radon shows radon removal on the order of 10^4 or more during the test period.

3.4. *Radon emanation*

The emanation of radon in Ag-zeolite samples was investigated. As measurement samples, we prepared 20 g samples each of an MFI zeolite without an Ag ion exchange and an MFI zeolite with an Ag ion exchange. Radon emanation is evaluated by observing the upwelling of radon over time from the zeolite. Measurements of each sample were performed independently. Each sample was placed in an FH, evacuated at 350°C, and circulated with purified G1-grade air at room temperature. Figure 8 shows the time profile of the radon emanation test with MFI (no Ag ion) and Ag-MFI. The time profile data of MFI were fitted as:

$$A(t) = A_{\mathrm{ema}}(1 - e^{-t/\tau}) + A_{\mathrm{BG}}e^{-t/\tau}, \tag{1}$$

where $A(t)$ is total radon rate, A_{ema} [mBq] is radon emanation rate, and A_{BG} [mBq] is remaining radon rate in the RD. $\tau = 3.8235/\ln 2$ [days] is the lifetime of ^{222}Rn. MFI has a large amount of emanation with A_{ema} ∼700 mBq/kg (14 mBq/20 g), whereas Ag-MFI has no significant emanation, as was the case with the other activated carbon adsorbent candidates [13]. This indicates that MFI itself has impurities containing radium, which produces radon, but in Ag-MFI, no radon is released due to its own ability to adsorb radon. It was determined that the current material, Ag-zeolite, is clean enough to produce less radon emanation than the approximate amount of radon emanation due to upwelling from the system, estimated by a separate measurement, ∼0.25 mBq for the system. Therefore, an Ag-zeolite made from the same material as the current Ag-zeolite sample shall be used for the air purification system.

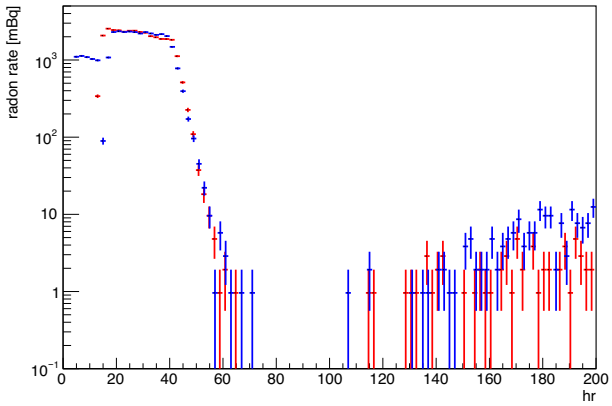

Fig. 9. The time profile of the radon rate during the radon removal test with an Ag-MFI sample (red) and one solidificated by PL-7 (blue).

3.5. *The adsorption performance of solidified Ag-zeolite*

The adsorption performance of Ag-zeolite solidified with a solidifier was evaluated. In the adsorption tests in Sections 3.2 and 3.3, Ag-zeolite was solidified as a pressed powder. However, considering the long-term stability of the zeolite filter, solidification with a solidifier is desirable. Therefore, a sample of Ag-MFI was solidified with 20 % colloidal silica (FUSO CHEMICAL CO., LTD. PL-7), 3 times its weight, at 350°C. As a result of the solidification process, the weight of the solidified sample increased by 50%. The solidified Ag-zeolite was crushed to a reasonable size from 0.7 to 2 mm, 30 g was placed in an FH, and the same procedure as in Section 3.2 was used for radon removal tests. Figure 9 shows the time profile of the radon counting rate during the radon removal test with the Ag-MFI sample and the one solidificated by PL-7. Although the increase in the radon counting rate after RnNO seems significant, no significant difference is found for the removal efficiency and the length of RnNO time. Therefore, solidification was found not to reduce adsorption efficiency. In the future, we aim to solidify a shaped product in order to guarantee adsorption efficiency in air purification systems.

3.6. *Effect of moisture on adsorption performance*

Furthermore, the effect of moisture on radon adsorption performance is as follows. The radon adsorption test with ambient air was resumed except for the nanoparticle filter which was blocked with impurities in Section 3.3. Thus, as in Section 3.3, the ambient air passes through 4A for moisture removal and then through Ag-zeolite. Figure 10 shows the results of the radon removal test after resuming. The dew point decreased immediately after reopening because the 4A was adsorbing moisture. Subsequently, the 4A became saturated and no longer adsorbed moisture, which allowed ambient air containing moisture to enter the Ag-zeolite and release radon. After this, the dew point increased and decreased once before reaching equilibrium. It is assumed that the radon that had previously been adsorbed is released, and at the same time, moisture is adsorbed onto the Ag-zeolite. The water and radon contents of the Ag-zeolite were determined from the time distributions of the dew point and radon content in Fig. 10, respectively. The details are discussed in the Appendix. As a result, 2×10^{22} water molecules (equivalent to 0.6 g) and 3×10^{7} radon atoms were estimated as the water and radon contents. After Rn was released, the sum of the amount of radon in the ambient air and the amount of radon released from the 4A [11] was observed. Therefore, air purification systems using Ag-zeolite

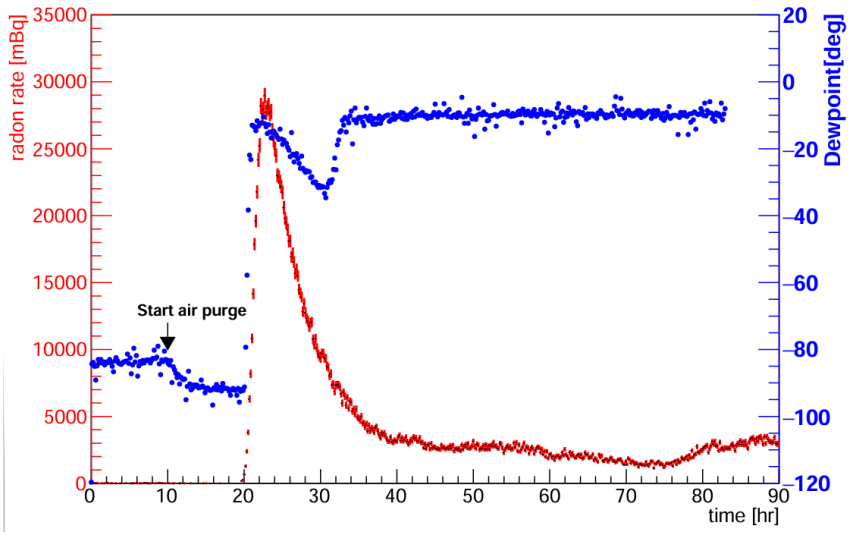

Fig. 10. The time profile of the radon counting rate (red) and dew point (blue) during the radon removal test by one pass after the nanoparticle filter was removed.

require measures such as removing sufficient moisture and radon from the Ag-zeolite in advance, monitoring the dew point and shutting down the system if moisture is introduced.

4. Conclusion

This paper investigates the removal of radon from purified and ambient airs by Ag-zeolite samples Ag-MFI and Ag-FER. The results show that the Ag-FER sample has radon removal on the order of 10^4 and has a higher adsorption capacity for radon than Ag-MFI. Sufficient radon removal capacity was confirmed not only in the case of air circulation, but also in the single-pass test, in which outside air is directly taken in. The adsorption capacity of Ag-zeolite for radon does not decrease when solidified with a solidifier. It was also found that there is almost no radon release from the Ag-zeolite itself, with release on the order of 0.1 mBq. Furthermore, it was found that the incorporation of water either reduced the ability to adsorb radon or rather released radon. These properties will be applied to the Hyper-Kamiokande experiment and to the development of air purification systems for ultra-low-radioactivity experiments.

Acknowledgements

This work was supported by Japan Society for the Promotion of Science (JSPS) KAKENHI Grant Number 23K03435, 19H05807, 24H02243 and the Inter-University Research Program of Institute for Cosmic Ray Research (ICRR), the University of Tokyo.

Data availability

Data available on request.

Appendix. Estimation of the amount of adsorbed water and released radon

Here are the details of the calculation of the amount of adsorbed water molecules and the amount of radon released in the Section 3.6 measurement.

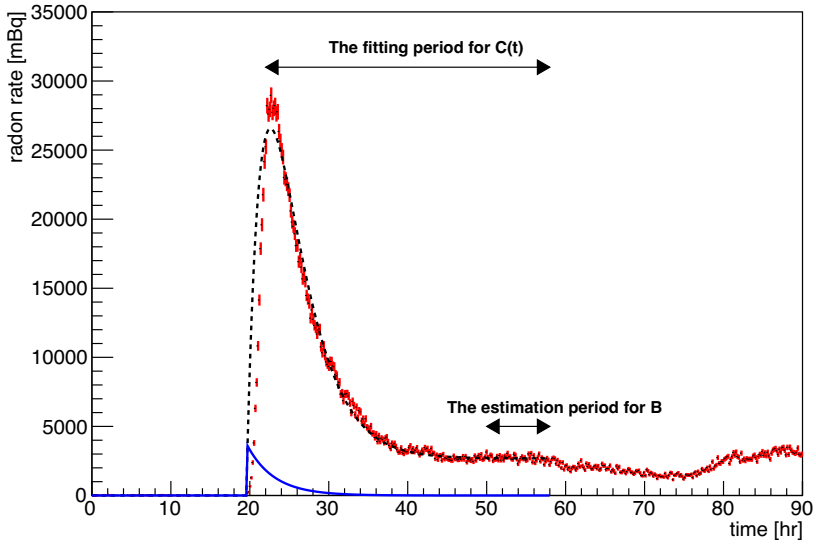

Fig. A1. The time profile of the radon counting rate (red). The assumed $A(t)$ (blue solid line) and $C(t)$ (black dashed line) for the best fit are also shown. The two arrows indicate the fitting period for $C(t)$ and the estimation period for B, respectively.

A.1. Amount of adsorbed water molecules

As shown in Fig. 10, immediately after moisture incorporation, the measured dew point of the dew point meter downstream of the Ag-zeolite dropped once and then reached equilibrium. The amount of moisture adsorbed during this period was derived by subtracting the amount of moisture determined from the dew point at each measurement point during this period from the average amount of moisture determined from the dew point at equilibrium over 40 hours in Fig. 10. The interval between each measurement point is 10 minutes, and the air flow rate at each measurement point is 5 L/10 min. The dew point was converted to moisture content using the table in Ref. [14]. The total amount of water adsorbed is determined to be 0.6 g, which corresponds to 2×10^{22} water molecules.

A.2. Amount of released radon

For the conversion of the amount of radon released from the Ag-zeolite, it is necessary to create a model that results in the time distribution of the amount of radon in Fig. 10 and derive it from there. The following two factors are taken into account.

First, the time distribution of radon released from the Ag-zeolite, $A(t)$, is defined as,

$$A(t) = A_0 e^{-(t-t0)/a}, \tag{A.1}$$

where A_0 is the amount of radon activity immediately after the release and a is the time constant of the release. t_0 is the start time of Rn release in Fig. 10 and is set to 19.6 hours. Next, the RD is 80 L, and air enters the detector passing the Ag-zeolite at 0.5 L/min and is released at 0.5 L/min to the outside. Let $C(t)$ be the activity of radon in the RD. Here, the time variation of $C(t)$ due to air entering and leaving the detector is

$$\frac{d\mathrm{C}(t)}{dt} = A(t) + B - \gamma \mathrm{C}(t), \tag{A.2}$$

where B is the amount of radon activity from the external air, assumed constant and obtained from the average of radon activity at $t = 50$–58 hours in Fig. 10. γ is the rate of release from the detector to the outside, with $\gamma = vdt/V$ (v: air flow rate 0.5 L/min, V: 80L).

In order to reproduce the radon release measurement data ($t = 22$–58 hours) in Fig. 10, A_0 and a in Eq. (A.1) are derived by fitting the time distributions of radon activity variables. The resulting graph is shown in Fig. A1. The derived $A(t)$ and $C(t)$ are shown here. To simplify the calculation of the estimates, we do not consider sequential equilibria of ^{222}Rn–^{214}Po for RD. The discrepancy between the measured data and the calculation at the rise around 20 hours may be attributed to this. From this result, it can be seen that $A_0 = 3590$(mBq) and $a = 3.4$(hours). The number of released radon atoms D is calculated by

$$D = \int A(t)dt/\lambda, \tag{A.3}$$

where λ is the decay coefficient for ^{222}Rn. As a result, $D = 3 \times 10^7$ was estimated.

References

[1] A. Ianni, SciPost Phys. Proc. **12**, 007 (2023).
[2] Y. Nakano, T. Hokama, M. Matsubara, M. Miwa, M. Nakahata, T. Nakamura, H. Sekiya, Y. Takeuchi, S. Tasaka, and R. A. Wendell, Nucl. Instrum. Methods Phys. Res. A **977**, 164297 (2020).
[3] K. Abe et al., Phys. Rev. D **109**, 092001 (2024).
[4] S. Fukuda et al., Nucl. Instrum. Methods Phys. Res. A **501**, 418 (2003).
[5] K. Abe et al., [arXiv:1805.04163[physics.ins-det], 28 Nov. 2018] [Search inSPIRE].
[6] Y. Takeuchi et al., Phys. Lett. B **452**, 418 (1999).
[7] Y. Nakano, H. Sekiya, S. Tasaka, Y. Takeuchi, R. A. Wendell, M. Matsubara, and M. Nakahata, Nucl. Instrum. Methods Phys. Res. A **867**, 108 (2017).
[8] M. Fukui et al., Xe adsorption performance of ag-loaded zeolite, in The 36th Zeolite Research Presentation (online) (The Zeolite Institute of Japan, 2020).
[9] S. Heinitz et al., Sci. Rep. **13**, 6811 (2023).
[10] O. Veselska, O. Llido, M.-C. Piro, S. Vaidya, S. Kusnicki, and J. Busto, Prog. Theor. Exp. Phys. **2024**, 023C01 (2024).
[11] H. Ogawa, K. Iyoki, M. Matsukura, T. Wakihara, K. Abe, K. Miuchi, and S. Umehara, J. Instrum. **19**, P02004 (2024).
[12] K. Hosokawa, A. Murata, Y. Nakano, Y. Onishi, H. Sekiya, Y. Takeuchi, and S. Tasaka, Prog. Theor. Exp. Phys. **2015**, 033H01 (2015).
[13] Y. Nakano, K. Ichimura, H. Ito, T. Okada, H. Sekiya, Y. Takeuchi, S. Tasaka, and M. Yamashita, Prog. Theor. Exp. Phys. **2020**, 113H01 (2020).
[14] Koganei Corp. Conversion from relative humidity to atmospheric dew point. Japan. https://official.koganei.co.jp/common/pdf/tech/E4041_volume_rate_conversion.pdf.